J. Inst. Eng. India Ser. B (June 2018) 99(3):235–243
https://doi.org/10.1007/s40031-017-0311-7

ORIGINAL CONTRIBUTION

An Enhanced Three-Level Voltage Switching State Scheme for Direct Torque Controlled Open End Winding Induction Motor

V. Praveen Kumar Kunisetti[1] · **Vinay Kumar Thippiripati**[1]

Received: 17 April 2017 / Accepted: 15 December 2017 / Published online: 15 January 2018

Abstract Open End Winding Induction Motors (OEWIM) are popular for electric vehicles, ship propulsion applications due to less DC link voltage. Electric vehicles, ship propulsions require ripple free torque. In this article, an enhanced three-level voltage switching state scheme for direct torque controlled OEWIM drive is implemented to reduce torque and flux ripples. The limitations of conventional Direct Torque Control (DTC) are: possible problems during low speeds and starting, it operates with variable switching frequency due to hysteresis controllers and produces higher torque and flux ripple. The proposed DTC scheme can abate the problems of conventional DTC with an enhanced voltage switching state scheme. The three-level inversion was obtained by operating inverters with equal DC-link voltages and it produces 18 voltage space vectors. These 18 vectors are divided into low and high frequencies of operation based on rotor speed. The hardware results prove the validity of proposed DTC scheme during steady-state and transients. From simulation and experimental results, proposed DTC scheme gives less torque and flux ripples on comparison to two-level DTC. The proposed DTC is implemented using dSPACE DS-1104 control board interface with MATLAB/SIMULINK-RTI model.

Keywords Direct torque control · Three-level inverter · Torque ripple · Open end winding induction motor · Switching-state scheme · Flux ripple

Introduction

Most popular methods to control the speed of induction motor drives are Field Oriented Control (FOC) [1] and Direct Torque Control (DTC) [2]. Implementation of FOC is quite complex since it involves co-ordinate transformation and rotor flux observer. The draw backs involved in the implementation of FOC can be overcome by using DTC. The scheme of DTC was introduced by Takahashi and Noguchi [2]. DTC offers high dynamic performance and it controls motor flux and torque directly by proper selection of voltage vectors. The limitations of DTC are higher ripples in torque, flux, variable switching frequency [3] and possible problems during low speeds of operation. Several research proposals are published to solve the problems of DTC. Torque and flux ripples of induction motor drive can be reduced by maintaining constant switching frequency. In order to maintain constant switching frequency space vector modulation based DTC (SVM-DTC) was introduced [4]. SVM-DTC provides less torque and flux ripples [4–8]. Implementation of SVM-DTC requires three PI controllers [4]. A novel SVM-DTC was implemented by using a PI controller and only one reference triangular wave [5]. A hybrid carrier based SVM-DTC is introduced for multi inverter fed induction motor drive; it involves co-ordinate transformation [6]. PI controllers used in SVM-DTC were replaced by intelligence algorithm the validity of this algorithm was shown by simulation only [8]. SVM-DTC requires computation of reference voltage space vector and tuning of PI controllers.

✉ V. Praveen Kumar Kunisetti
kvpraveenkumar15@gmail.com

[1] Electrical Engineering Department, National Institute of Technology, Warangal 506004, Telangana, India

Torque and flux ripples of induction motor drive can be reduced by using dithering [9]. Dithering involves high frequency carrier signals and a PI controller; which may increases complexity of DTC. Constant Switching Frequency Controller (CSFC) is introduced to replace 3-level torque hysteresis controller in DTC [10]. CSFC improvises the performance of Induction Motor Drive (IMD) even at zero and low speeds. DTC of three-level NPC inverter fed IMD was introduced to reduce torque ripples by decreasing distortions in current [11]. An adaptive nonlinear DTC technique was implemented with loss-minimization strategy but it requires high speed processor [12]. PI controllers used in conventional DTC were replaced with Type-2 fuzzy controllers [13] to improve dynamic performance of OEWIM drive. In [14], neuro-fuzzy controller is implemented for IM drive with simple tuning algorithm. Low cost DTC for induction motor is implemented without using current sensors [15]. This algorithm is simple, robust and less expensive but it does not account limitations of DTC. A low speed high torque motor drive with modular multi-level cascaded converter based on triple-star bridge cells is developed. It provides numerical analysis of common mode current and DC-capacitor voltage [16]. The novel load angle control based DTC is developed by earlier researchers [17]. This method reduces torque and flux ripple during steady-state and transient states. This method requires an angle estimator.

From the literature survey, it is evident that torque ripple of induction motor drive can be reduced by using SVM or multi-level inverter fed IMD. Implementation of SVM-DTC is quite complex so multi-level inversion fed DTC is preferable to reduce torque and flux ripples. DTC of four-level VSI was introduced by cascading three two-level inverters [18] and it involves 18 switches for its operation. Multilevel inversion with dual inverter fed OEWIM drive attains prominent status owing to its merits: simple structure, elimination of clamping diodes in Neutral Point Clamped (NPC) inverters, elimination of flying capacitors, less number of DC sources [19]. In [20] DTC of OEWIM was implemented with dual inverter configuration. SVM-DTC of OEWIM drive was implemented by operating the two inverters with equal DC link voltages [21]. In [22] DTC of OEWIM is implemented by 12-sided polygonal active voltage vectors.

In this article, the scheme of DTC is developed for OEWIM without using SVM technique. OEWIM is suitable for electric vehicles [23], ship propulsion [24] and easy inclusion of PV arrays [25]. Electric vehicles and ship propulsion applications require ripple free torque, hence in this paper the main focus is laid to reduce torque ripple. The three-level inversion is obtained by using dual inverter fed OEWIM configuration. The objectives of the proposed scheme are: (1) Implementing an enhanced voltage switching scheme for OEWIM drive to reduce torque and flux ripples. (2) Reducing problems during low speeds of operation. (3) Reducing the problems during sudden variations of speed. (4) Selection of active voltage vectors based on rotor speed. (5) Operating the OEWIM drive with constant V/f ratio. The effectiveness of proposed DTC scheme verified experimentally with dSPACE DS-1104 control board.

Control Method of Proposed DTC

The block diagram of proposed dual inverter fed OEWIM drive is shown in Fig. 1a. In the block diagram, ω_r^* is reference speed (rad/s), ω_r is actual speed of rotor (rad/s), T_e^* is reference torque (N-m) obtained from PI controller, T_e is actual torque (N-m), $|\psi_s^*|$ is stator flux reference (Wb), ψ_s is actual flux (Wb), θ_s is angle of flux linkages, V_{dc} is input DC voltage of VSI, i_a, i_b and i_c are motor phase currents.

Power Circuit of OEWIM

The configuration of OEWIM drive is shown in Fig. 1b, the motor is supplied with the difference of voltages obtained from two inverters. Three-level inversion was obtained by operating two inverters with equal DC-link voltage. The advantage of OEWIM configuration is it uses two inverters and they are operated with half of the rated DC-link voltage. Table 1 shows the realization of voltage space vectors used to implement proposed DTC algorithm. Switches are turned 'ON', to realize switching states to obtain three-level output voltage. In Fig. 1c, there are 18 non-zero voltage vectors (V_1–V_{18}). The active vectors are shown in Fig. 1c. Hence the three-level inverter produces 18 active voltage space vector locations.

Following is an example to determine resultant space vector for switching combinations of (1,0,0) and (0,1,1) for inverters 1 and 2. Where '1' refers to top switch of respective VSI is ON,'0' indicates lower switch of respective VSI is ON. The output voltages of inverters are given by Eqs. (1) and (2). The voltage space vector V_s is obtained from difference of output voltages of inverter-1 and inverter-2.

$$V_{01} = \frac{2}{3} * \frac{V_{dc}}{2}\left(S_a + S_b e^{j\frac{2\pi}{3}} + S_c e^{j\frac{4\pi}{3}}\right) \quad (1)$$

$$V_{02} = \frac{2}{3} * \frac{V_{dc}}{2}\left(S'_a + S'_b e^{j\frac{2\pi}{3}} + S'_c e^{j\frac{4\pi}{3}}\right) \quad (2)$$

$$\text{and} \quad V_s = (V_{01} - V_{02}) \quad (3)$$

From Eq. (3), the obtained voltage space vector has magnitude of V_{dc}, that is vector V_7.

Similarly, if the switching combinations are (1,1,0) and (0,1,0) then obtained voltage space vector has magnitude

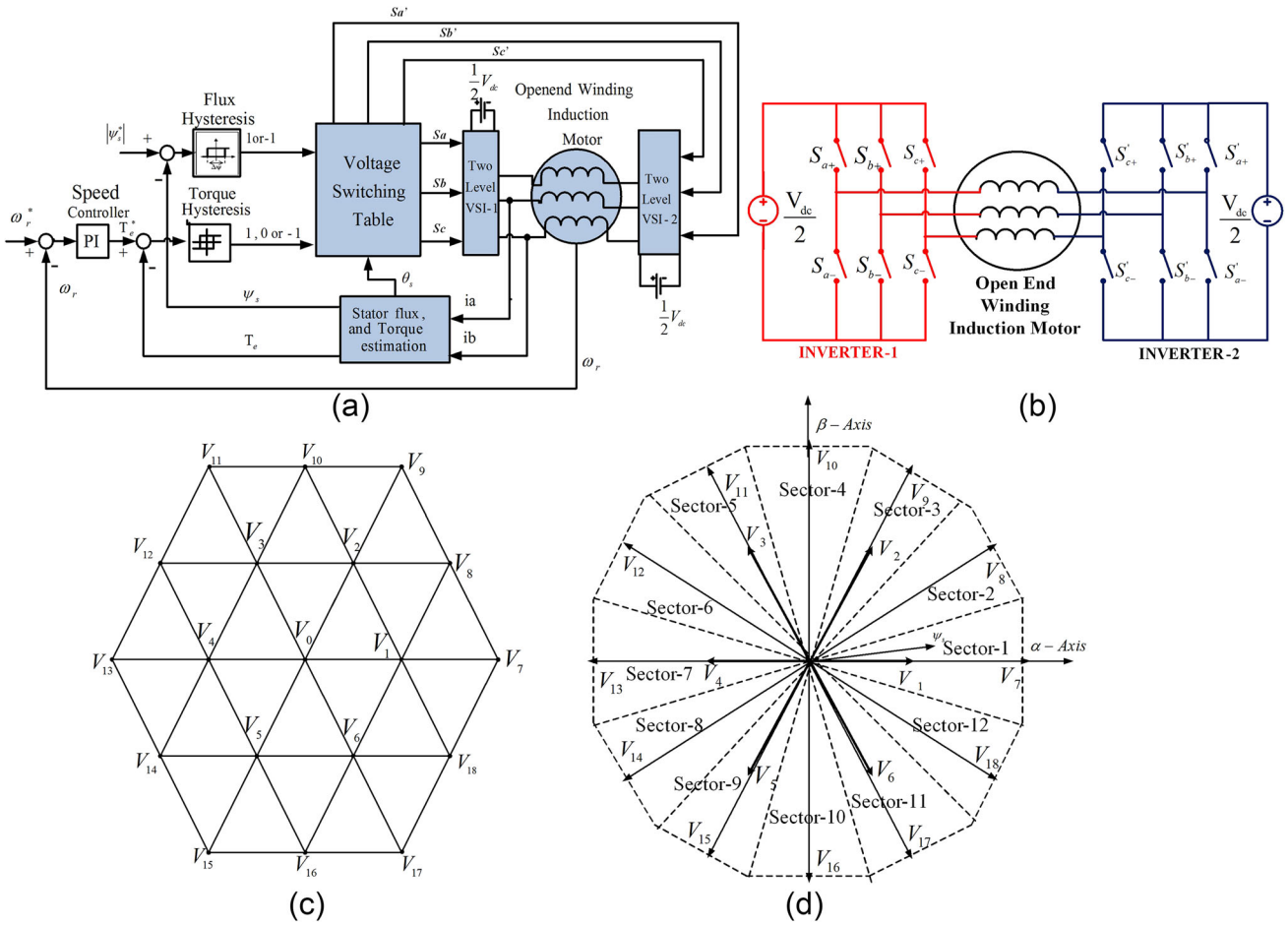

Fig. 1 **a** Block diagram of proposed DTC, **b** power circuit diagram, **c** voltage space vectors and **d** classification of sectors

$V_{dc}/2$, and it is named as V_1. On arranging all the vectors it forms like a hexagon and it is shown in Fig. 1d, further the voltage space vectors are divided into 12-sectors. Sector-1 occupies (345^0–15^0) with respect to α-axis. Sector-2 is from (15^0–45^0). Sector-3 is from (45^0–75^0). Sector-4 is from (75^0–105^0). Sector-5 is from (105^0–135^0). Sector-6 is from (135^0–165^0). Sector-7 is from (165^0–195^0). Sector-8 is from (195^0–225^0). Sector-9 is from (225^0–255^0). Sector-10 is from (255^0–285^0). Sector-11 is from (285^0–315^0) and sector-12 is from (315^0–345^0). From space vector diagram, the voltage vectors are categorized into two groups. Voltage vectors V_7–V_{18} are used to operate at higher frequencies (more than *66% of* ω_r). Voltage space vectors V_1–V_6 are used to operate the drive with low (less than *33% of* ω_r) and medium (between low–high) frequencies.

High Frequency of Operation

The voltage space vectors V_7–V_{18} and a null vector V_0 are used to control torque and flux of OEWIM drive for high frequencies of operation. In Fig. 1d, if the location of stator flux is in sector-1 then the voltage space vectors V_8, V_9, V_{17} and V_{18} are applied to increase its magnitude, whereas the voltage space vectors V_{11}, V_{12}, V_{14} and V_{15} are applied to reduce its magnitude. For sector-1 to reduce positive torque error V_8, V_9 and V_{10} are utilized, whereas to reduce negative torque error V_{16}, V_{17} and V_{18} are utilized. In this mode of operation V_1–V_6 should not be used and selection of vectors is given in Table 2. By utilizing the voltage vectors V_7–V_{18} three-level output voltage can be obtained.

Medium and Low Frequency of Operation

The voltage vectors V_1–V_6 and null-vector V_0 are used to control torque and flux of OEWIM drive for medium and low frequencies. In Fig. 1d, if the location of stator flux vector is in sector-I then the active voltage vectors V_2 and V_6 are applied to increase its magnitude, whereas the voltage vectors V_3 and V_5 are applied to decrease its magnitude. In sector-1 to reduce positive torque error V_2 is utilized, whereas to reduce negative torque error V_5 is utilized. In this mode of operation V_7–V_{18} should not be used selection of vectors is given in Table 3. By utilizing the voltage vectors V_1–V_6 two-level output voltage can be obtained.

Table 1 Switching states of inverters 1 and 2

Inverter-1			Inverter-2			Voltage space vectors	Realization		Output voltage level
S_a	S_b	S_c	S_a'	S_b'	S_c'	V_s	Magnitude	Angle (°)	
1	1	0	1	1	0	V_0	0	0	Space vectors V_1–V_6, delivers two-level output voltage
1	1	0	0	1	0	V_1	$0.333*V_{dc}$	0	
0	1	0	0	1	1	V_2	$0.333*V_{dc}$	60	
0	1	1	0	0	1	V_3	$0.333*V_{dc}$	120	
0	0	1	1	0	1	V_4	$0.333*V_{dc}$	180	
1	0	1	1	0	0	V_5	$0.333*V_{dc}$	− 120	
1	0	0	1	1	0	V_6	$0.333*V_{dc}$	− 60	
1	0	0	0	1	1	V_7	$0.667*V_{dc}$	0	Space vectors V_7–V_{18}, delivers three-level output voltage
1	1	0	0	1	1	V_8	$0.5774*V_{dc}$	30	
1	1	0	0	0	1	V_9	$0.667*V_{dc}$	60	
0	1	0	0	0	1	V_{10}	$0.5774*V_{dc}$	90	
0	1	0	1	0	1	V_{11}	$0.667*V_{dc}$	120	
0	1	1	1	0	1	V_{12}	$0.5774*V_{dc}$	150	
0	1	1	1	0	0	V_{13}	$0.667*V_{dc}$	180	
0	0	1	1	0	0	V_{14}	$0.5774*V_{dc}$	− 150	
0	0	1	1	1	0	V_{15}	$0.667*V_{dc}$	− 120	
1	0	1	1	1	0	V_{16}	$0.5774*V_{dc}$	− 90	
1	0	1	0	1	0	V_{17}	$0.667*V_{dc}$	− 60	
1	0	0	0	1	0	V_{18}	$0.5774*V_{dc}$	− 30	

Table 2 Switching table of proposed three-level DTC for high speeds

Flux error	Torque error	Sector											
		1	2	3	4	5	6	7	8	9	10	11	12
1	1	V_9	V_{10}	V_{11}	V_{12}	V_{13}	V_{14}	V_{15}	V_{16}	V_{17}	V_{18}	V_7	V_8
	− 1	V_{17}	V_{18}	V_7	V_8	V_9	V_{10}	V_{11}	V_{12}	V_{13}	V_{14}	V_{15}	V_{16}
− 1	1	V_{11}	V_{12}	V_{13}	V_{14}	V_{15}	V_{16}	V_{17}	V_{18}	V_7	V_8	V_9	V_{10}
	− 1	V_{15}	V_{16}	V_{17}	V_{18}	V_7	V_8	V_9	V_{10}	V_{11}	V_{12}	V_{13}	V_{14}

Table 3 Switching table of proposed three-level DTC for low and medium speeds

Flux error	Torque error	Sector											
		1	2	3	4	5	6	7	8	9	10	11	12
1	1	V_2	V_2	V_3	V_3	V_4	V_4	V_5	V_5	V_6	V_6	V_1	V_1
	− 1	V_6	V_6	V_1	V_1	V_2	V_2	V_3	V_3	V_4	V_4	V_5	V_5
− 1	1	V_3	V_3	V_4	V_4	V_5	V_5	V_6	V_6	V_1	V_1	V_2	V_2
	− 1	V_5	V_5	V_6	V_6	V_1	V_1	V_2	V_2	V_3	V_3	V_4	V_4

Reduction of Torque and Flux Ripple

The voltage ripple has direct impact on performance of OEWIM drive. Torque and flux ripples are dependent on voltage ripple. The output voltage of inverter is given by

$$v(t) = R_s i_s + L_s \frac{di_s}{dt} + e_0 \tag{4}$$

where $v(t)$ is the output voltage of three level inverter, and it has 18 voltage space vectors shown in Table 2. e_0 is the EMF induced and it depends on frequency of operation. L_s is self-inductance and i_s is current. On neglecting stator voltage drop in Eq. (4), can be rewritten as

$$\frac{di_s}{dt} = \left(\frac{v(t) - e_0}{L_s}\right) \tag{5}$$

From Eq. (5), it is evident that the rate of change of stator current is dependent on selection of inverter voltage vector for the respective operating frequency. Hence to get low current ripple at steady state, it is required to select suitable voltage vector which maintains di_s/dt as minimum. The rate change of stator current is dependent on inverter voltage vector and back EMF. Therefore di_s/dt is independent of rotor flux magnitude. Since the rotor time constant is much high when compared to stator time constant. The choice of active voltage vectors to reduce torque and flux ripples are shown in Tables 2 and 3.

Figure 2 represents the deviation of current ripple for high and low frequencies of operation. Figure 2a gives the selection of voltage vector for high frequency of operation by assuming the flux space vector is in sector-I. Figure 2b represents selection and impact of voltage vectors for low and medium frequencies. If the flux space vector is in sector-1 by applying vector V_{10} rather than vector V_9 it results in higher change of load angle. Hence, V_{10} should not be applied. To reduce torque and flux errors V_9 should be applied. For low and medium operating frequencies, if flux space vector is in sector-1 then voltage vector V_9 should not be applied to increase torque and flux, because it increases current ripple di_s/dt. For low and medium frequencies voltage vector V_2 should be applied. By applying V_9 and V_2 for high and medium range of frequencies, it maintains constant V/f ratio.

Experimental Results

The proposed three-level DTC is implemented by using dSPACE-1104 control board with MATLAB/SIMULINK real time interface. An experiment is conducted on OEWIM drive to show the effectiveness of proposed DTC algorithm at various rotor speeds. In interest of brevity, experimental results are shown for low (100 rad/s), medium (200 rad/s) and high frequencies (300 rad/s) of operation in forward and reverse motoring. Figure 3 represents actual speed and flux of OEWIM drive for two-level and proposed three-level DTC respectively. Figure 3a, b represent actual speed and flux of motor in forward motoring for step change in speed variations of 100, 200 and 300 rad/s. Figure 3c, d represent speed and flux of motor in reverse motoring for speed variations of − 100, − 200 and − 300 rad/s. Figure 3e, f represent flux locus of two-level and proposed DTC, respectively. From Fig. 3, it is evident that the proposed three-level DTC gives less flux ripple when compared with two-level DTC and it provides better dynamic response for high speed variations.

Figure 4 represents speed and torque of OEWIM drive for two-level and proposed three-level DTC respectively. Figure 4a, b represent actual speed and torque of motor in forward motoring for step change in speed variations of 100, 200 and 300 rad/s. Figure 4c, d represent actual speed and torque of OEWIM drive for the speed variations of − 100, − 200 and − 300 rad/s. Figure 4e, f represent actual speed and torque of OEWIM drive for the speed variation from 100 to 200 rad/s and 100 rad/s. The steady-state torque ripple in proposed DTC algorithm is very less when compared with two-level inversion.

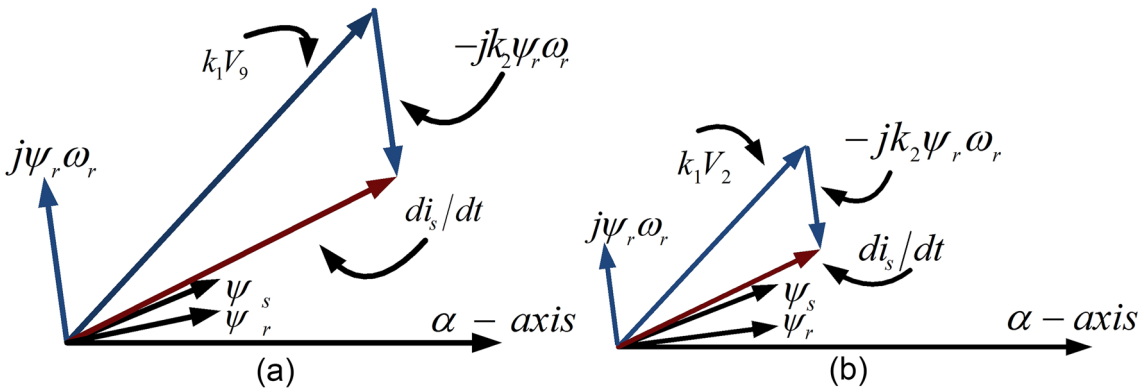

Fig. 2 Rate of change of stator current to increase flux and torque for: **a** high Speeds and **b** low speeds

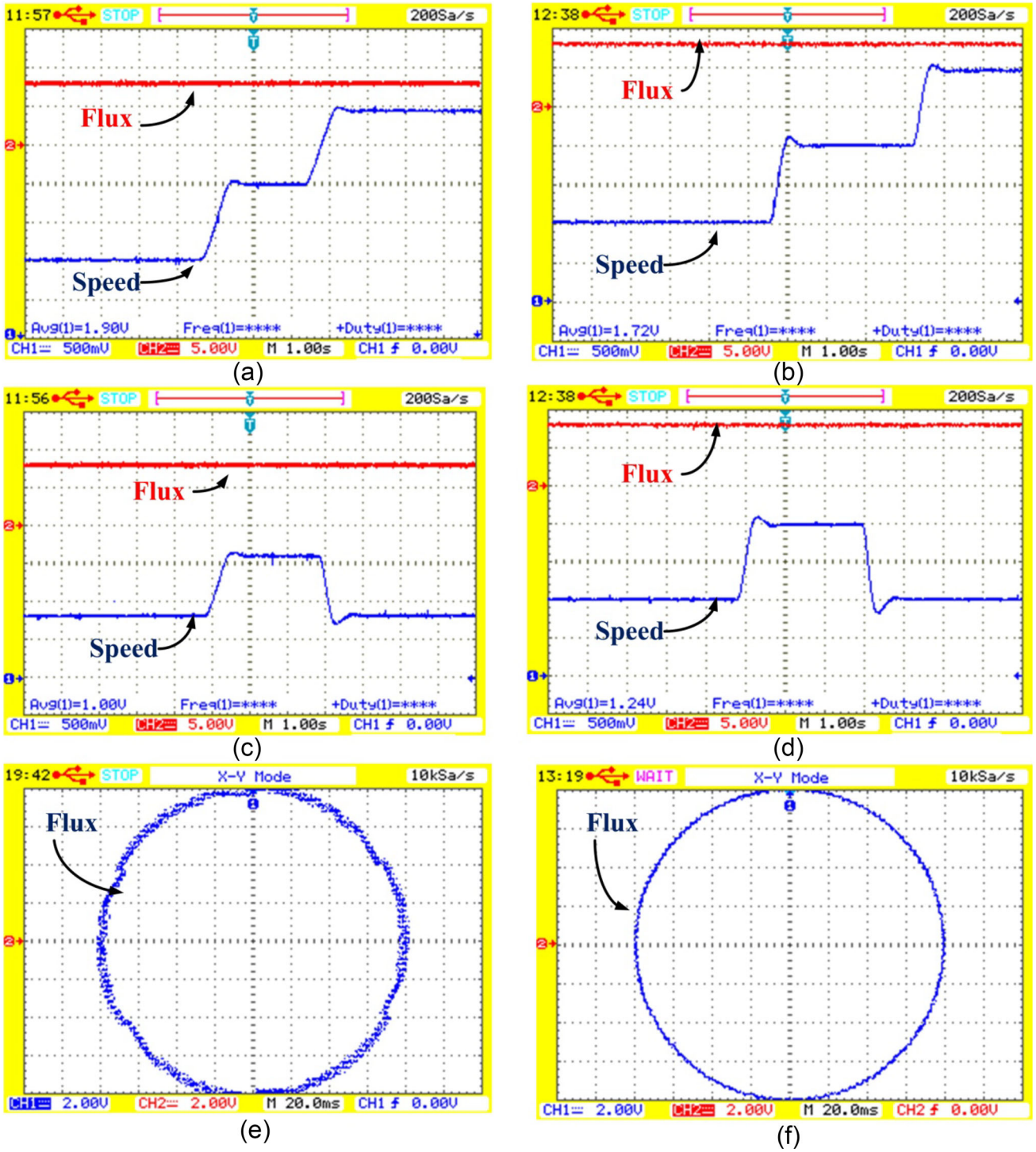

Fig. 3 Experimental results of two-level and proposed DTC: **a** speed and flux in forward motoring, **b** speed and flux in forward motoring, **c** speed and flux for variation of speed, **d** speed and flux for variation of speed (Speed@50 rad/s/div), (Flux@0.5 Wb/div). **e** Flux locus, **f** flux locus (0.2 Wb/div)

Figure 5a, b represent a-phase voltage of OEWIM drive and Common Mode Voltage (CMV) of two-level DTC. Figure 5c, d represent a-phase voltage of OEWIM drive and CMV of proposed DTC. Figure 5e, f represent a-phase current of OEWIM drive for two-level and proposed DTC respectively. Figure 5g represents quantified torque ripple under steady state condition at different operating frequencies. From Fig. 4, it is clear that the

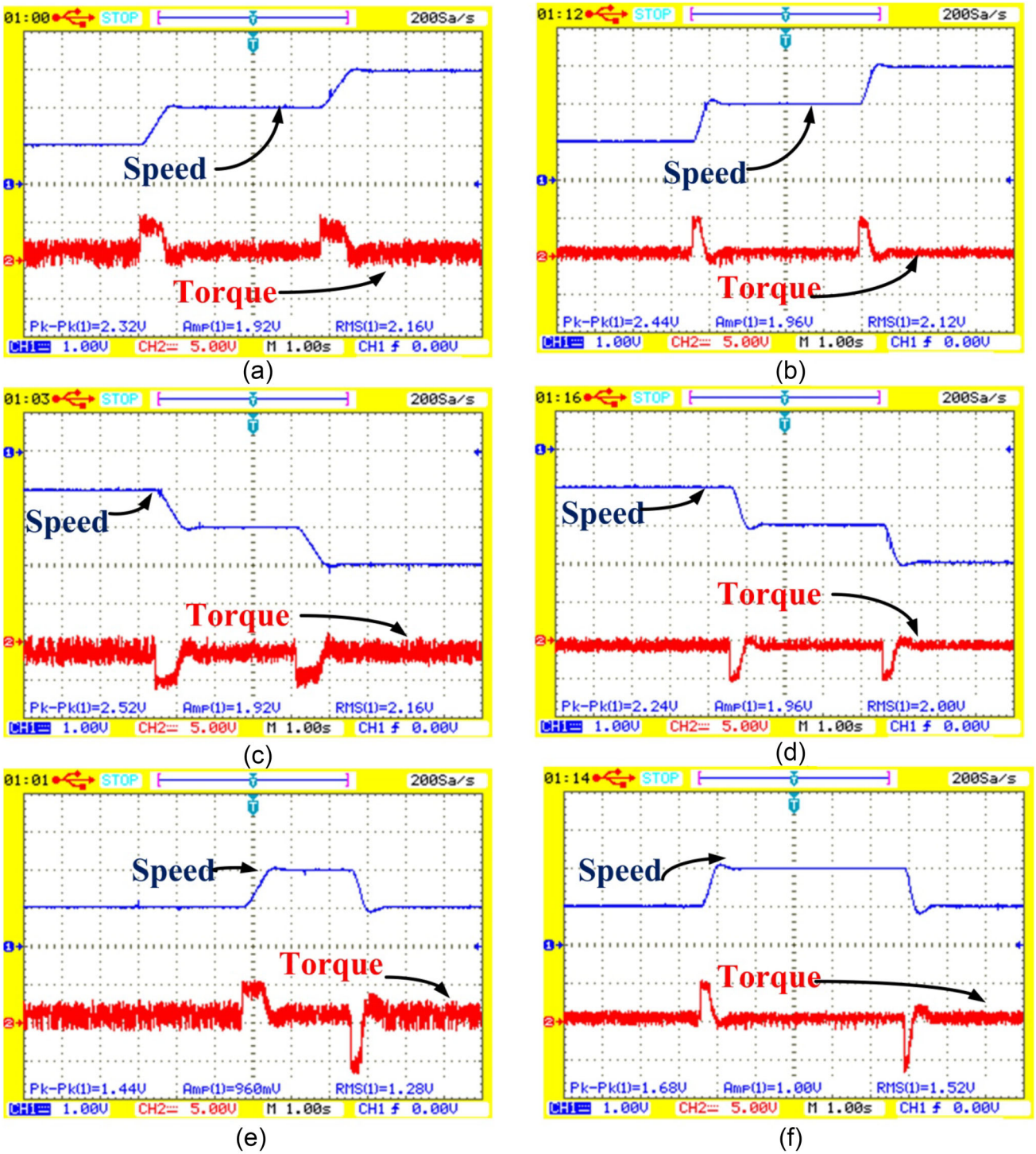

Fig. 4 Experimental results of two-level and proposed DTC: **a** speed and torque in forward motoring, **b** speed and torque in forward motoring, **c** speed and torque in reverse motoring, **d** speed and torque in reverse motoring, **e** speed and torque for variation of speed from 100 to 200 rad/s, **f** speed and torque for variation of speed from 100 to 200 rad/s (Speed@100 rad/s/div), (Torque@5 N-m/div)

proposed-three level DTC gives less torque ripple when compared with two-level DTC for all operating speeds, for brevity only three speeds of operation is reported in this article.

Conclusion

In this article, a modified three-level voltage switching scheme is implemented for OEWIM drive with the help of two two-level inverters to reduce torque and flux ripples at

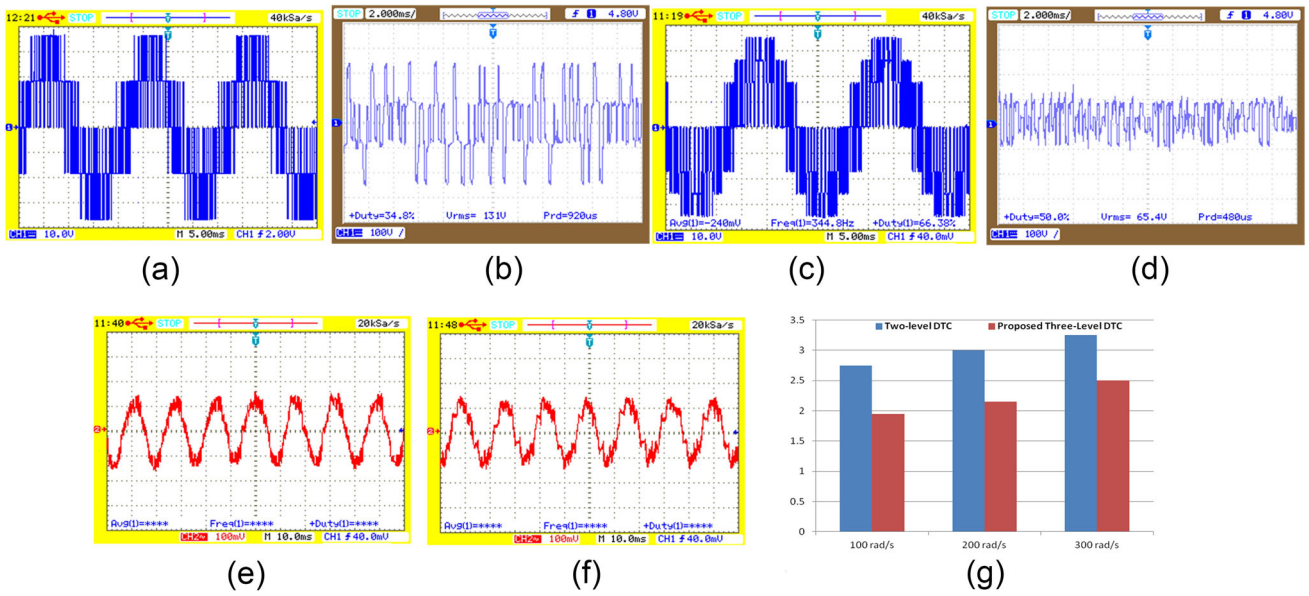

Fig. 5 Experimental results @ 300 rad/s: **a** voltage/phase: 100 V/div, **b** CMV for two-level configuration, **c** voltage/phase: 100 V/div, **d** CMV of proposed DTC, **e** current/phase of two-level DTC, **f** current/phase of proposed DTC (1 A/div) and **g** steady-state torque ripple

different speed conditions. The proposed scheme is closer to conventional DTC, so it gives all the features of DTC. The two two-level inverters are operated with individual DC sources, so it is easy to interface with PV arrays. The intents of this article are: (1) implementing an effective voltage switching state scheme for an OEWIM, (2) classification of voltage vectors based on rotor speed, (3) reducing the problems encountered at low speeds and (4) limiting the ripples in torque and flux. The effectiveness of proposed algorithm was verified experimentally by operating OEWIM in forward and reverse motoring at low (100 rad/s), medium (200 rad/s) and high (300 rad/s) speeds. The future scope of the proposed article is to implement for multilevel configuration using unequal DC supplies and implementing with the help of predictive control. From hardware results, proposed three-level DTC gives less torque and flux ripples when compared with two-level DTC for all speeds of operation.

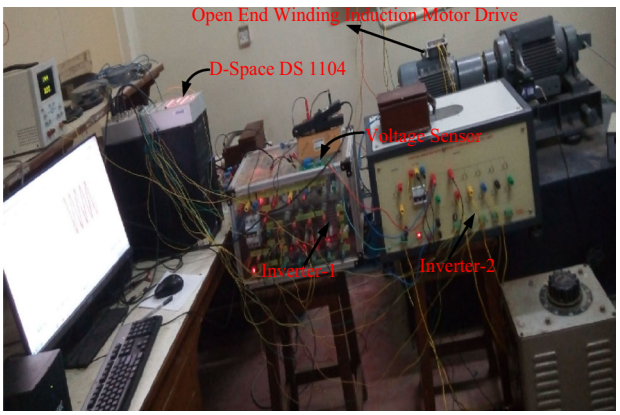

Fig. 6 Experimental set-up

Appendix

The photo graph consists of 4-pole, 3-phase, 415 V, 7.54 A, 1440 RPM, 5 H.P OEWIM drive. The motor is fed with 2-VSI's and operated with isolated DC sources. The rated speed of motor drive is 1440 RPM (300 rad/s in terms of Electrical Frequency). The motor is tested at low, medium and high frequencies in forward and reverse motoring modes. Switching pulses for the inverters are given by dSPACE-1104 control board and it is synchronized with MATLAB/SIMULINK (Fig. 6).

References

1. D. Casadei, F. Profumo, G. Serra, A. Tani, FOC and DTC: two viable schemes for induction motors torque control. IEEE Trans. Power Electron. **17**(5), 779–787 (2002)
2. I. Takahashi, T. Noguchi, A new quick-response and high-efficiency control strategy of an induction motor. IEEE Trans. Ind. Appl. **22**(5), 820–827 (1986)
3. D. Telford, M.W. Dunnigan, B. W. Williams, A comparison of vector control and direct torque control of an induction machine, in *Conference Proceedings: IEEE PESC'00*, Galway, pp. 421–426 (2000)
4. T.G. Habetler, F. Profumo, M. Pastorelli, L.M. Tolbert, Direct torque control of induction machines using space vector modulation. IEEE Trans. Ind. Appl. **28**(5), 1045–1053 (1992)
5. X. Zhang, G.H.B. Foo, A constant switching frequency-based direct torque control method for interior permanent-magnet

synchronous motor drives. IEEE/ASME Trans. Mechatron. **21**(3), 1445–1456 (2016)
6. T.V. Kumar, S.S. Rao, Modified direct torque control of three phase induction motor drives with low ripple in flux and torque. Leonardo J. Sci. (LJS) **10**(18), 27–44 (2011)
7. U.V. Patil, H.M. Suryawanshi, M.M. Renge, Closed-loop hybrid direct torque control for medium voltage induction motor drive for performance improvement. IET Power Electron. **7**(1), 31–40 (2014)
8. B. Kirankumar, Y.V. Siva Reddy, M. Vijayakumar, Multilevel inverter with space vector modulation: intelligence direct torque control of induction motor. IET Power Electron. **10**(10), 1129–1137 (2017)
9. T. Noguchi, M. Yamamoto, S. Kondo, I. Takahashi, Enlarging switching frequency in direct torque-controlled inverter by means of dithering. IEEE Trans. Ind. Appl. **35**(6), 1358–1366 (1999)
10. I.M. Alsofyani, N.R.N. Idris, Simple flux regulation for improving state estimation at very low and zero speed of a speed sensorless direct torque control of an induction motor. IEEE Trans. Power Electron. **31**(4), 3027–3035 (2016)
11. S. Mukherjee, G. Poddar, Direct torque control of squirrel cage induction motor for optimum current ripple using three-level inverter. IET Power Electron. **3**(6), 904–914 (2010)
12. M. Hajian, J. Soltani, G.A. Markadeh, S. Hosseinnia, Adaptive nonlinear direct torque control of sensorless IM drives with efficiency optimization. IEEE Trans. Ind. Electron. **57**(3), 975–985 (2010)
13. N.V.R. Naik, S.P. Singh, Improved torque and flux performance of type-2 fuzzy-based direct torque control induction motor using space vector pulse width modulation. Electr. Power Compon. Syst. **42**(6), 658–669 (2014)
14. M. Hafeez, M.N. Uddin, N.A. Rahim, H.W. Ping, Self-tuned NFC and adaptive torque hysteresis-based DTC scheme for IM drive. IEEE Trans. Ind. Appl. **50**(2), 1410–1420 (2014)
15. B. Metidji, N. Taib, L. Baghli, T. Rekioua, S. Bacha, Low-cost direct torque control algorithm for induction motor without AC phase current sensors. IEEE Trans. Power Electron. **27**(9), 4132–4139 (2012)
16. W. Kawamura, K.L. Chen, M. Hagiwara, H. Akagi, A low-speed, high-torque motor drive using a modular multilevel cascade converter based on triple-star bridge cells (MMCC-TSBC). IEEE Trans. Ind. Appl. **51**(5), 3965–3974 (2015)
17. T.V. Kumar, S.S. Rao, Hardware implementation of direct load angle controlled induction motor drive. Electr. Power Compon. Syst. **42**(14), 1505–1516 (2014)
18. T.V. Kumar, S.S. Rao, Direct torque controlled induction motor drive based on cascaded three two-level inverters. Int. J. Model. Simul. **34**(2), 70–82 (2014)
19. L. Suresh, S. Nagarjun, V.T. Somasekhar, Improvised SVPWM strategies for an enhanced performance for a four-level open-end winding induction motor drive. IEEE Trans. Ind. Electron. **64**(4), 2750–2759 (2017)
20. K.V. Praveen Kumar, T. Vinay Kumar, Experimental implementation of direct torque control of open end winding induction motor, in *Conference Proceedings: IEEE-TENCON*, Singapore, pp. 3318–3323 (2016). https://doi.org/10.1109/TENCON.2016.7848666
21. A.Kumar, B.G.Fernandes, K.Chatterjee, Direct torque control of open-end winding induction motor drive using the concept of imaginary switching times for marine propulsion systems, in *Conference Proceedings: IEEE-PESC-04*, vol. 2, pp. 1214–1219
22. C. Patel, P.P. Rajeevan, A. Dey, R. Ramchand, K. Gopa Kumar, M.P. Kazmeirkowski, Fast direct torque control of open end induction motor drive using 12-sided polygonal voltage space vectors. IEEE Trans. Power Electron. **27**(1), 400–410 (2012)
23. A.D. Kiadehi, K.E.K. Drissi, C. Pasquier, Angular modulation of dual-inverter fed open-end motor for electrical vehicle applications. IEEE Trans. Power Electron. **31**(4), 2980–2990 (2016)
24. S. Lu, K. Corzine, Multilevel multi-phase propulsion drives, in *Conference Proceedings: IEEE Electric Ship Technologies Symposium (ESTS)*, Philadelphia, pp. 363–370 (2005)
25. S. Jain, R. Karampuri, V.T. Somasekhar, An integrated control algorithm for a single-stage PV pumping system using an open-end winding induction motor. IEEE Trans. Ind. Electron. **63**(2), 956–965 (2016)